Macromolecules

ARTICLE

pubs.acs.org/Macromolecules

The Origin of Heterogeneity of Polymer Dynamics near the Glass Temperature As Probed by Defocused Imaging

Ania Deres,[†] George A. Floudas,[‡] Klaus Müllen,[§] Mark Van der Auweraer,[†] Frans De Schryver,[†] Jörg Enderlein,[⊥] Hiroshi Uji-i,[*,†] and Johan Hofkens[*,†]

[†]Department of Chemistry, Katholieke Universiteit Leuven, Celestijnenlaan 200 F, 3001 Heverlee, Belgium

[‡]Department of Physics, University of Ioannina, 45110 Ioannina, Greece, and Foundation for Research and Technology-Hellas, Biomedical Research Institute

[§]Max-Planck-Institut für Polymerforschung, Ackermannweg 10, D-55128 Mainz, Germany

[⊥]Drittes Physikalisches Institut, Universität Göttingen, Friedrich-Hund-Platz 1, D-37077 Göttingen, Germany

Supporting Information

ABSTRACT: Single molecule defocused wide-field fluorescence microscopy (SMDWM) has been used to monitor the 3D reorientation of single molecules in a thin polymer film (~300 nm) of monodisperse poly(*n*-butyl methacrylate) near the glass temperature (T_g). Stroboscopic illumination allows for estimating reliable correlation times of single molecule rotational diffusion owing to the drastic lengthening of the observable trajectories. We demonstrate that homogeneity is restored ~19 K above the T_g determined with calorimetry. The rotational correlation times obtained from SMDWM show similar temperature dependence as the ones measured with established bulk measurements, such as dielectric spectroscopy and rheology, on the same polymer sample. Single molecular reorientation is coupled to the segmental rather than terminal relaxation of the surrounding polymer matrix. SMDWM revealed that spatial heterogeneity is more pronounced than temporal heterogeneity within the measurement time scale (hours to days), whereas this information is hidden in the bulk measurement.

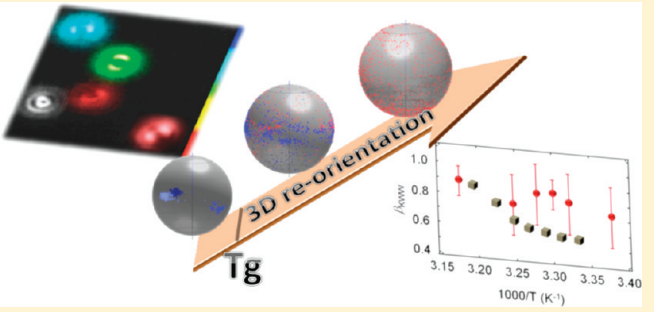

Dynamics of polymers near the glass transition temperature (T_g) are complex due to their heterogeneous nature.[1−9] It is well-known that the dynamic properties of polymers, such as viscosity or segmental and terminal relaxation time, vary over several orders of magnitude in frequency/time on approaching the glass temperature. Despite intensive research on this phenomenon for several decades, a clear, molecular scale explanation of the liquid-to-glass transformation is still missing. Nevertheless, there is consensus that the aforementioned processes are linked to the structural relaxation known as the α-relaxation, reflecting the intra- and intermolecular cooperativity of polymer segments. This process exhibits highly nonexponential behavior especially in the vicinity of T_g. Although the origin of the nonexponential behavior is still under debate, two extreme cases have been considered.[2,3] The first hypothesis suggests that heterogeneous environments are responsible as, locally, relaxation processes are purely exponential but the time constants vary in space. Averaging over many molecules with different relaxation times gives rise to the observed nonexponential behavior (spatial heterogeneity). Alternatively, the second mechanism assumes that the system is spatially homogeneous but the local structure relaxes nonexponentially (temporal heterogeneity). In the former case a pertinent question is over what length scales the spatial heterogeneity extends, while for the latter scenario the question is how often the dynamics exchange.

The nonexponential relaxation dynamics have been experimentally observed by various ensemble techniques, such as multidimensional NMR,[10,11] dielectric spectroscopy,[12−17] fluorescence anisotropy,[18,19] and fluorescence recovery after photobleaching[20] as well as by various single molecule based methods.[1,7,8,21−37] It is hard to pinpoint the exact nature of the observed heterogeneity with conventional ensemble techniques, as many molecules are averaged over both time and space. In contrast, single molecule spectroscopy (SMS) has the potential to provide a deeper insight, since this technique allows monitoring individual molecules separately, thus avoiding ensemble averaging. Following the rotational diffusion of individual single molecules embedded in a polymer matrix has been proven to be useful in studying local polymer dynamics.[1,7,8,21−37] The rotational diffusion of the embedded molecules is assumed to report on the structural relaxation of the surrounding matrix under the premise that single

Received: June 25, 2011
Revised: September 21, 2011
Published: November 07, 2011

Scheme 1. Chemical Structures of Perylene Derivatives: (a) 1, (b) 2, and (c) PnBMA

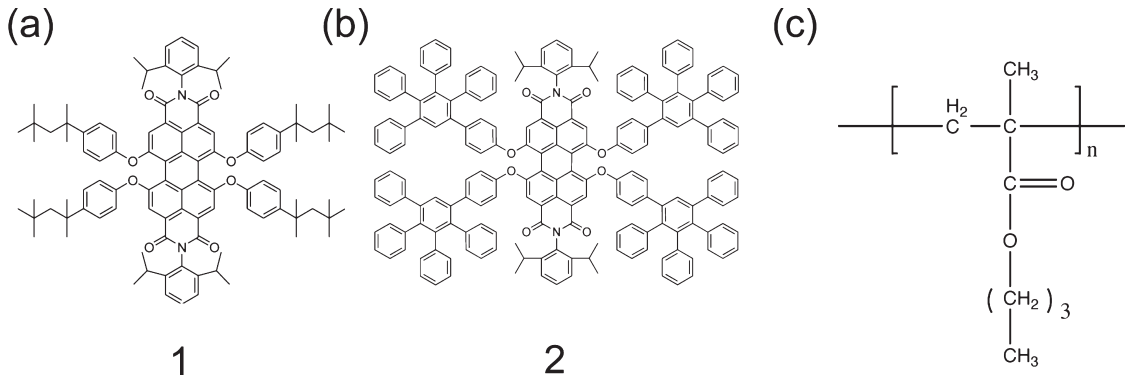

molecules can hardly change their orientations independently from the surrounding polymer matrix.[1,31−36]

In this contribution, we apply defocused wide-field fluorescence microscopy (SMDWM) in a detailed study of the rotational diffusion of single molecules embedded in poly(*n*-butyl methacrylate) (PnBMA) films with a thickness of ∼300 nm. The main advantage of defocused wide-field microscopy is its ability to visualize the full 3D evolution of the orientation of individual single molecules in a single image of many square micrometers *in parallel* (see also the Supporting Information sections 1 and 2 for the details on the defocused imaging).[36−41] By taking sequential defocused images, we have shown in previous publications that one can obtain rotational correlation times of many molecules simultaneously.[36,40,41] The rotational correlation time that can be calculated from the observed reorientations of individual molecules can then be linked to local polymer relaxation. This massive parallel detection scheme allows for the eventual observation of spatial and temporal heterogeneities simultaneously. However, the reorientational trajectory lengths of single molecules, even those of the most robust dye molecules such as rylene derivatives,[42,43] are limited in time by irreversible photobleaching. Consequentially, the trajectories are often not long enough to compute reliable correlation times. Since the polymer relaxation near T_g is often a very slow process, relevant relaxation times can be very long. Vanden Bout and co-workers recently have shown, by both experimental and theoretical studies, that the trajectory lengths have to be more than 100−1000 times longer than the correlation time of the system under study if one wants to extract correct information.[44,45] However, the survival time of the fluorescent probe is usually in the order of minutes under normal excitation conditions of SMS.[46] In order to overcome this limitation, we adopted an approach based on defocused imaging that is often used in single molecule microscopy to lengthen substantially a single molecule's survival time, namely the use of stroboscopic illumination. Next, we obtained single molecule correlation times at various temperatures above T_g and compared those with the ones obtained from ensemble techniques, i.e., rheology and dielectric spectroscopy (DS). We established a nearly identical temperature dependence for the single molecule and ensemble derived measurements. This bench marking is crucial in establishing that single molecule measurements can indeed accurately be used to follow the polymer relaxation. Furthermore, we confirm that the molecular rotation of single molecule reorientations is sensitive to the structural (segmental) relaxation rather than to the terminal relaxation. Finally, our data allowed us to discuss and visualize spatial heterogeneity of diffusive motions at different temperatures, with a spread in time over several orders of magnitude.

■ TEMPERATURE DEPENDENCE OF SINGLE-MOLECULE ROTATIONAL RELAXATION

The temperature dependence (*T*-dependence) of the rotational diffusion of a perylene diimide derivative, **1** (Scheme 1a), in a PnBMA (Scheme 1c) (M_w = 10 200 g/mol, M_w/M_n = 1.06, Polymer Source, Inc.) film is monitored with defocused imaging at temperatures around the glass temperature (T_g ∼ 296 K as determined by differential scanning calorimetry (second heating run with 10 K/min)). The temperature range explored extends from T_g to T_g + 19 K. Figure 1a−c displays typical trajectories for the in-plane angle (ϕ), the out-of-plane angle (θ), and the 3D angular displacement (Φ) for individual molecules of **1** as a function of time at 296, 308, and 315 K, respectively. The corresponding 3D projection maps are presented in Figure 1d−f. As expected, larger angular displacements were detected at higher temperatures. More importantly, the molecular reorientation dynamics show characteristic properties which depend on the temperature at which they are monitored. At and below 296 K, the dye molecules tend to be locked in a preferential orientation and only occasionally show a sudden reorientation (rotational jump), as shown in Figure 1a,d by changing the color of the observed Φ values. In contrast, consecutive changes of molecular reorientation with relatively larger angular displacements are observed at higher temperatures, for example at 315 K. The 3D projection map displays a nearly full coverage of angular space by the probe over time, without any detectable preferential orientation (Figure 1f). At 308 K (i.e., T_g + 12 K), an intermediate behavior is observed: the probe molecule exhibits exchange between slow (locked orientation) and fast dynamics (large amplitude 3D reorientations). During the first 250 s (red in Figure 1b,e), the probe shows relatively fast rotational diffusion in all directions, which is similar to the behavior at 315 K. After 250 s (blue in Figure 1b,e), the probe shows rotational diffusion characterized by periods of limited motion and occasional jumps into different orientations. The observed exchange dynamics have been correlated previously with temporal heterogeneous relaxation of the surrounding polymer chains.[1,31−36] With increasing temperature, the time scale of the trapped state decreases in favor of the fast diffusion, which indicates that the system changes from heterogeneous to a homogeneous behavior progressively with increasing temperature.

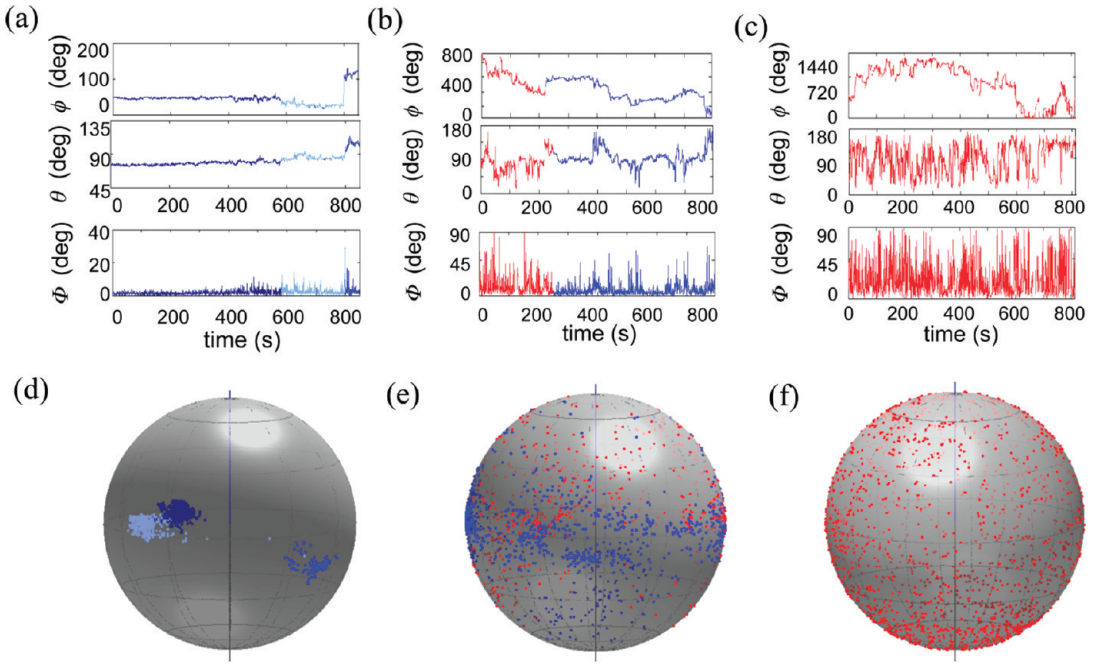

Figure 1. Temperature dependence of rotational diffusion behavior of **1** in a PnBMA thin film. In- and out-of-plane and 3D representation angles as a function of time at 296 K (a), 308 K (b), and 315 K (c) and the corresponding 3D projection map (d–f).

STROBOSCOPIC ILLUMINATION: ACCURATE RELAXATION TIME ESTIMATION WITH SINGLE MOLECULE MICROSCOPY

The rotational correlation time of individual molecules was estimated by performing an autocorrelation of the 3D reorientation, Φ, of the probe molecules, which is done by calculating the time average, ⟨cos(Φ)⟩ (for details on SMDWM at different temperatures and analysis, see Supporting Information). The correlation time can be properly estimated only when the trajectories are long enough. According to the simulation results reported by Vanden Bout et al.,[44,45] the trajectory length should be 100−1000 times longer than the actual correlation time. This means that extremely long trajectories are needed for accurate estimation of the relaxation times of individual molecules at a given temperatures near T_g because polymer relaxation is usually very slow in this temperature regime. Although rylene dyes have been reported to perform very well in single molecule studies in terms of long-term imaging (survival times of up to an hour under typical single molecule excitation conditions have been reported),[1,36,37,42,43] in order to extract reliable relaxation times, even longer trajectories are required. Herein, to lengthen the observation window of the single molecule trajectories, we employed a stroboscopic illumination approach. A lag time was introduced between each frame, and the laser illumination was synchronized with the image frame rate. In this way, the probe molecules are not exposed to the excitation light between frames, resulting in a reduced photobleaching rate and thus significantly longer trajectories (from typical several minutes to several hours in the stroboscopic approach with a lag time of 4.8 s). Note that close to T_g it is not necessary to monitor the reporter molecule continuously since molecules are trapped in certain orientations for times longer than the lag time as they follow the slow structural relaxation (see Figure 1a). As the dynamics drastically change in a small temperature interval near T_g, the lag time for each temperature has to be determined from the relaxation behavior of the

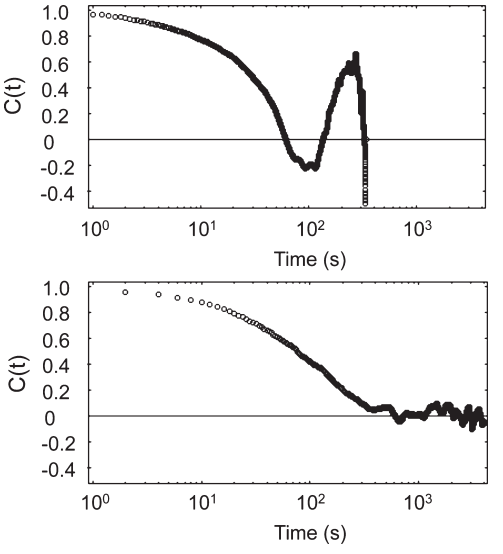

Figure 2. Effect of the stroboscopic illumination approach on the observed rotational autocorrelation function of a single molecule: (a) the correlation function as a function of time with an imaging rate of 5 Hz without a lag time; (b) the autocorrelation function of trajectory obtained with an imaging rate of 0.25 Hz with 200 ms integration time and 3.8 s lag time.

autocorrelation function. The effect of the stroboscopic illumination can be clearly seen in the correlation function depicted in Figure 2. In the absence of the lag time, the autocorrelation function of a trajectory at an image rate of 5 Hz shows poor statistics and even drops to negative values before fully relaxing. On the other hand, introducing a lag time of 4.8 s together with an integration time of 200 ms for each frame (imaging rate of 0.2 Hz) results in a correlation function with excellent statistics and a smooth approach to zero. This indicates that the length of the trajectories

dx.doi.org/10.1021/ma201449p |*Macromolecules* 2011, 44, 9703–9709

Table 1. KWW Fitting Parameters and Calculated Correlation Times, τ_c, Obtained from Fluorescence Spectroscopy Measurements with the Values of N Describing the Percentage of Molecules for Which the Correlation Times Have Been Calculated at Each Temperature and L Being the Trajectory Length

T [K]	N [%]	t_{lag} [s]	$\langle\tau_c\rangle$ [s]	$\langle\tau_{KWW}\rangle$ [s]	$\langle\beta_{KWW}\rangle$	$L/\langle\tau_c\rangle$
296	20	14.8	767 ± 289	640 ± 244	0.72 ± 0.19	91
301	72	4.8	141 ± 94	112 ± 61	0.78 ± 0.23	177
303	81	4.8	69 ± 19	59 ± 19	0.84 ± 0.12	360
305	81	1.8	43 ± 14	37 ± 14	0.83 ± 0.24	207
308	75	1.8	17 ± 10	12 ± 8	0.75 ± 0.18	538
315	86	0	5 ± 2	5 ± 2	0.88 ± 0.12	484

is statistically sufficient for estimating an accurate correlation time (Figure 2b). The corresponding correlation time for the depicted example was estimated to be 126 s (β_{KWW} = 0.88, τ_{KWW} = 119 s). As expected, a shorter lag time is required for higher temperatures. For example, we estimated lag times to be typically ~4.8 s at 301 K and ~0.8 s at 308 K. In conclusion, using the stroboscopic approach, the trajectory length can easily fulfill the requirement of being 100 times longer than the extracted correlation time (see Table 1).

The values of $\langle\tau_c\rangle$ were determined by averaging the values obtained from nearly 100 molecules for each temperature except for the temperature being equal to 296 K. At 296 K, only a limited number of molecules (~20% of all molecules) showed a full relaxation of their autocorrelation function even for trajectories recorded for over 30 h, due to the extremely slow dynamics at this temperature. At higher temperatures, the correlation function exhibits a relaxation to zero for more than 70% of molecules seen in the field of view. The obtained values of the fitting parameters and correlation times are presented in the Table 1. The correlation times vary by 2 orders of magnitude in the temperature range from 296 to 315 K while the obtained β_{KWW} values (a measure for the nonexponential behavior) increase from 0.72 to 0.88 in the same temperature range, indicating less nonexponential behavior at higher temperatures.

COMPARISON WITH ENSEMBLE MEASUREMENTS

The size of the fluorescent molecules usually used in fluorescence spectroscopic techniques, owning to their extended conjugated framework, is larger than the dimensions of the polymer repeat units. Under this premise an obvious question is how accurately the molecular dynamics of the probe are reporting on the polymer dynamics. In view of the significance of the structural polymer relaxation for the liquid-to-glass transformation, it is natural to search for a correlation between the probe dynamics and the polymer segmental dynamics.[3,24] This is relevant as the time scale of cooperative motions—like the α-relaxation—corresponds well with the time scale accessible by single molecule experiments (milliseconds to hours). In order to validate the use of the defocused wide-field imaging for studying polymer relaxation and for pinpointing the particular relaxation process of PnBMA, we decided to benchmark the single molecule data against the established bulk techniques of dielectric spectroscopy (DS)[12−17] and rheology.[4,47] The result of the comparison is displayed in Figure 3, where the ensemble-average relaxation times obtained from DS and rheology are plotted side to side with the results obtained from SMS on the same polymer sample (experimental details on both methods in the Supporting Information).

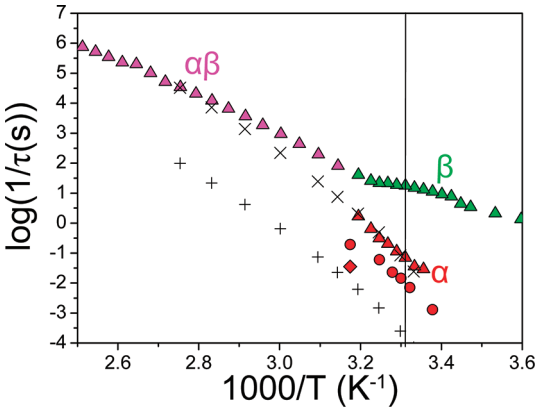

Figure 3. Arrhenius diagram for PnBMA representing a comparison between single molecule and bulk studies. Three relaxation processes are shown based on the analyses of the dielectric spectra; α (red triangles), β (green triangles), and $\alpha\beta$ (magenta triangles). The symbols + and × indicate terminal and segmental relaxations obtained from rheology measurements, respectively. Filled circles represent the correlation time calculated from single molecule studies for **1** and filled rhombus for **2**. The α-relaxations obtained from bulk and single molecule experiments clearly have very similar temperature dependencies.

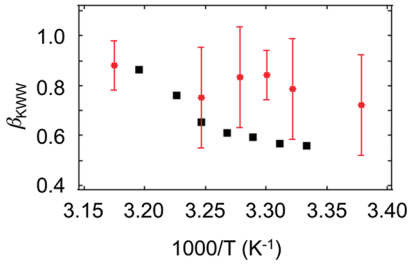

Figure 4. Calculated β_{KWW} parameters from the two shape parameters used in DS (filled black square) as well as the same parameter obtained from SM experiments (filled red circle).

From the viscoelastic measurements, the segmental and terminal relaxation times were obtained. The extracted shift factors display a temperature dependence that is depicted in the Arrhenius plot shown in Figure 3. Both shift factors display a strong T-dependence associated with the structural (α-) and longest chain relaxations. In the same figure we include three out of four measured dielectrically active processes (the γ process is discussed in Supporting Information, see Figure S4). At low temperature, the β-process with the Arrhenius T-dependence ($\tau = \tau_0 \exp(E/RT)$) and with activation parameters $\tau_0 = 1.6 \times 10^{-13}$ s and E = 67 kJ/mol shows a dielectric strength that is increasing function of temperature at the expense of the slower (α-) process. On the other hand, the α-process shows a strong T-dependence that is in good agreement with the Vogel−Fulcher−Tammann (VFT) equation. Unfortunately, the T-range is too small to get reliable parameters. Nevertheless, the dielectric α-process times are nearly identical to the segmental relaxation times as obtained from rheology. At even higher temperatures, the α- and β-processes merge to a single $\alpha\beta$-process that can be described by the VFT equation

$$\tau_{max} = \tau_0 \exp\left(\frac{B}{T - T_0}\right) \quad (2)$$

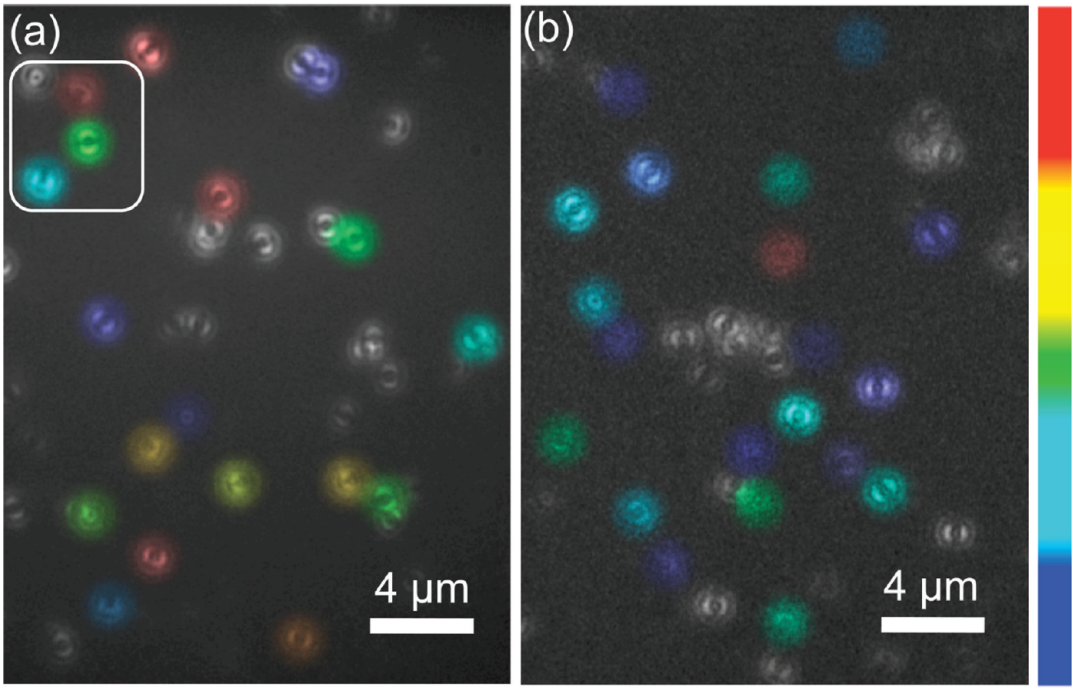

Figure 5. Mapping of spatial heterogeneity at 296 K (a) and at 315 K (b). The color coding represents the degree of deviation of individual molecular correlation times from the average value obtained of all analyzed single molecules.

where T_0 (= 178 K) is the ideal glass temperature, $\tau_0 = 1.66 \times 10^{-13}$ s, and $B = 3500 \pm 300$ K is the activation parameter.

Figure 3 includes the correlation times extracted from SMS measurements and reported in Table 1. The good agreement between the latter times for the dielectrically active α-process as well as the T-dependence of the corresponding relaxation times suggests that the dye molecules are following the structural relaxation of the polymer. Indeed, it has been suggested that rotational diffusion of molecules embedded in a polymer film monitors α-relaxation using bulk measurements, such as dielectric spectroscopy and nonlinear laser spectroscopy. This time scale is slower by a factor of ~6 compared to the α-relaxation segmental relaxation and faster by 1 order of magnitude than the terminal relaxation as obtained, respectively, from dielectric spectroscopy and rheology. This further suggests that the effective local friction that the dye is sensing corresponds quite well to that of a segment. We mention here that advanced NMR techniques[11] revealed extended backbone chain conformations, with conformational memory, as the units involved in the structural relaxation of poly(*n*-alkyl methacrylates). The origin of the motion was the randomization/isotropization of extended chain segments, comprising 5−10 repeat units that was promoted by the local structure in poly(*n*-alkyl methacrylates). Interestingly, the time scale of the dye rotational diffusion is in the proximity of this process.

The slower time scale extracted from SMDWM can be explained by the fact that the size of the probe molecule may influence its response to the polymer chain motion. It is likely that more than one segments are required to make the individual probes reorient. In fact, the correlation time of the bigger probe molecule, **2**, with a size that is ~2 times larger than of **1**, is significantly slower (filled rhombus in Figure 3 at 315 K). This probe-size dependence is consistent with the reports by Ediger et al.[20] and Kaufman et al.[48] It is worth to mention again that both the relaxation times of smaller and bigger probes are shorter than the relaxation time attributed to the terminal motion of PnBMA chains, which strongly supports the hypothesis that individual single probe molecules sense the segmental relaxation process rather than the terminal relaxation process.

The distributions of the correlation parameters, β_{KWW}, as estimated by DS and SMDWM shows a different T-dependence: while the β_{KWW} value obtained from DS displays a strong T-dependence, the corresponding parameter obtained from SMDWM is less sensitive to temperature variations and shows substantially higher average values (Figure 4). For homogeneous diffusion, the autocorrelation function would yield a single exponential decay, i.e., $\beta_{KWW} = 1$. The averaged values from single molecule experiments exhibit weaker temperature dependence, but the distribution at each temperature is remarkably broad. This may suggest that in the time scale of the observation temporal heterogeneities do not make the main contribution to the observed nonexponential relaxation observed in DS. Instead, spatial heterogeneities seem to be dominant. Indeed, if temporal heterogeneity would be the main contribution, all observed single molecules should have a low β_{KWW} value. In the DS measurements one averages spatially over many contributing molecules, resulting in the observed temperature dependence of β_{KWW}. This convincingly demonstrates that one can resolve the temporal and spatial contributions in the observed heterogeneous relaxation of polymers close to T_g using SMDWM. The contribution of the two distinct relaxation mechanisms is obviously obscured in any bulk measurements due to the ensemble averaging.

■ MAPPING OF SPATIAL HETEROGENEITY

As a proof of the above statement, we can analyze the rotational diffusion of a set of molecules in one field of view in SMDWM. Different individual single molecules show indeed rotational diffusion behavior in a broad range of time scales. This observation represents direct proof of the aforementioned spatial

heterogeneity. The fast dynamics of polymer relaxation can be monitored in real time at high imaging frame rate. Note that this, in contrast to the aforementioned stroboscopic approach, results in relative (to the full relaxation) short time trajectories. The correlation function of Φ on a fast time scale has been analyzed using a simplified way, namely by an isotropic rotational model, yielding $C(t) \sim \exp(-2Dt)$. If the rotational diffusion is not dynamically heterogeneous, the correlation function should reveal a single-exponential decay. $C(t)$, however, does not show a pure single-exponential decay but rather a biexponential decay as a result of the small temporal contribution to the heterogeneity. This contribution is attributed to the exchange dynamics observed during the short measurement interval, as shown in Figure 1 as well as in our previous study.[36] In order to directly compare the dynamics of different single molecules at different temperatures, normalization is required, since the absolute values of the relaxation times vary by several orders of magnitude in vicinity of T_g. Here, we propose a method that is similar to determining a relative error of the diffusion constants. For this purpose, the deviation was calculated, where D is the diffusion constant of a given single molecule and $\langle D \rangle$ is the mean value of the diffusion constants as averaged over all molecules observed at a given temperature. Subsequently, the absolute values of $r_e = (D - \langle D \rangle)/\langle D \rangle$ for individual single molecules are mapped in space using false color coding. Figures 5a and 5b show typical examples of the mapping with a field of view of $18 \times 24\ \mu m^2$ at 296 and 315 K, respectively. The color bar displays the value of r_e, i.e., of diffusion coefficients. The change from blue to red corresponds to a change from a small to a large value of the deviation from the averaged value (which was estimated from more than 100 molecules at each temperature). First of all, a narrower distribution of the deviation is found at 315 K. Most of the molecules show diffusion constants close to the average value. In contrast, in the map for 296 K, higher deviation values (orange to red) are found. Interestingly, as indicated by the white square in Figure 5a, even though the separation is only $1-2\ \mu m$ between molecules, a broad distribution of deviation values can be found. This result further underlines the notion that polymer dynamics vary on (sub)micrometer length scales (spatial heterogeneity). For the molecules that are presented in white in Figure 5, it was impossible to calculate a diffusion constant due to a limited trajectory length.

CONCLUSIONS

Temporally and spatially heterogeneous relaxation dynamics of glass-forming materials near the glass transition temperature have been monitored by observing rotational diffusion of embedded individual single molecules using defocused wide-field fluorescence microscopy. Employing a stroboscopic excitation scheme, the duration of single molecule reorientation trajectories can be extended to over hundred times the value of the relaxation correlation time, which allows for avoiding artifacts caused by insufficient statistics. The obtained correlation times of single molecules show a similar temperature dependence as the one observed in bulk measurements using established techniques such as dielectric relaxation (DS). Moreover, comparison between SMDM and rheology made on the same polymer sample revealed that the observed single molecular rotations are coupled to the segmental polymer relaxation rather than to the terminal processes. A statistical method based on the deviation of individual correlation times from their average value has been proven to be useful when discussing the temperature dependence of the spatial heterogeneity. Although both temporal and spatial heterogeneity were found in the polymer matrix in the vicinity of the glass temperature, spatial heterogeneity seems to be more relevant for the observed dynamics on the observation time scale in the studied polymer PnBMA. Furthermore, it was shown that homogeneity is restored some ~19 K above the DSC T_g at the time scale of the SMDM measurements. In conclusion, we have shown that defocused single molecule imaging is a powerful tool to unravel the molecular origin of heterogeneous polymer dynamics near the glass temperature.

ASSOCIATED CONTENT

Supporting Information. Details of the wide-field single-molecule microscopy setup, details of defocused imaging and image analysis, and data analysis on rheology and dielectric spectroscopy. This material is available free of charge via the Internet at http://pubs.acs.org.

AUTHOR INFORMATION

Corresponding Author

*E-mail: hirsohi.ujii@chem.kuleuven.be (H.U.), johan.hofkens@chem.kuleuven.be (J.H.).

ACKNOWLEDGMENT

The authors thank the "Fonds voor Wetenschappelijk Onderzoek FWO" (Grants G.0402.09, G0413.10, G0697.11, G0197.11), the K.U. Leuven Research Fund (GOA 2011/03, Center of Excellence INPAC, CREA2007, CREA2009 "Interdisciplinair Onderzoek" IDO/07/010), the Flemish government (Long term structural funding - Methusalem funding CASAS METH/08/04), and the Federal Science Policy of Belgium (IAP-VI/27) for financial support. H.U. thanks the Japanese Society for the promotion of Science and Technology (JST) for a PRESTO grant.

REFERENCES

(1) Wöll, D.; Braeken, E.; Deres, A.; De Schryver, F. C.; Uji-i, H.; Hofkens, J. *Chem. Soc. Rev.* **2009**, *38* (2), 313–328.
(2) Ediger, M. D.; Angell, C. A.; Nagel, S. R. *J. Phys. Chem.* **1996**, *100* (31), 13200–13212.
(3) Ediger, M. D. *Annu. Rev. Phys. Chem.* **2000**, *51*, 99–128.
(4) Zondervan, R.; Xia, T.; van der Meer, H.; Storm, C.; Kulzer, F.; van Saarloos, W.; Orrit, M. *Proc. Natl. Acad. Sci. U. S. A.* **2008**, *105* (13), 4993–4998.
(5) Hiwatari, Y.; Miyagawa, H.; Odagaki, T. *Solid State Ionics* **1991**, *47* (3–4), 179–222.
(6) Odagaki, T. *Phys. Rev. Lett.* **1995**, *75* (20), 3701–3704.
(7) Vogelsang, J.; Brazard, J.; Adachi, T.; Bolinger, J. C.; Barbara, P. F. *Angew. Chem., Int. Ed.* **2011**, *50* (10), 2257–2261.
(8) Kulzer, F.; Xia, T.; Orrit, M. *Angew. Chem., Int. Ed.* **2010**, *49* (5), 854–866.
(9) Richert, R. *J. Phys.: Condens. Matter* **2002**, *14* (23), R703–R738.
(10) Schmidt-Rochr, K.; Spiess, H. W. *Multi-dimensional Solid-State NMR and Polymers*; Academic Press: London, 1994.
(11) Wind, M.; Graf, R.; Heuer, A.; Spiess, H. W. *Phys. Rev. Lett.* **2003**, *91* (15), 155702.
(12) Dixon, P. K.; Wu, L.; Nagel, S. R.; Williams, B. D.; Carini, J. P. *Phys. Rev. Lett.* **1990**, *65* (9), 1108–1111.
(13) McCrum, N. G.; Read, B. E.; Williams, G. *Anelastic and Dielectric Effects in Polymeric Solids*; Dover Publications: New York, 1991.

(14) Garwe, F.; Schönhals, A.; Beiner, M.; Schroter, K.; Donth, E. *J. Phys.: Condens. Matter* **1994**, *6* (35), 6941–6945.
(15) Kremer, F.; Schoenhals, A. *Broadband Dielectric Spectroscopy*; Springer: Berlin, 2002.
(16) Floudas, G.; Mpoukouvalas, K.; Papadopoulos, P. *J. Chem. Phys.* **2006**, *124* (7), 074905.
(17) Mpoukouvalas, K.; Floudas, G.; Williams, G. *Macromolecules* **2009**, *42* (13), 4690–4700.
(18) Viovy, J. L.; Monnerie, L.; Merola, F. *Macromolecules* **1985**, *18* (6), 1130–1137.
(19) Ediger, M. D. *Annu. Rev. Phys. Chem.* **1991**, *42*, 225–250.
(20) Cicerone, M. T.; Blackburn, F. R.; Ediger, M. D. *Macromolecules* **1995**, *28* (24), 8224–8232.
(21) Link, S.; Hu, D.; Chang, W. S.; Scholes, G. D.; Barbara, P. F. *Nano Lett.* **2005**, *5* (9), 1757–1760.
(22) Vallée, R. A. L.; Marsal, P.; Braeken, E.; Habuchi, S.; De Schryver, F. C.; Van der Auweraer, M.; Beljonne, D.; Hofkens, J. *J. Am. Chem. Soc.* **2005**, *127* (34), 12011–12020.
(23) Vallée, R. A. L.; Van Der Auweraer, M.; De Schryver, F. C.; Beljonne, D.; Orrit, M. *ChemPhysChem* **2005**, *6* (1), 81–91.
(24) Cherdhirankorn, T.; Floudas, G.; Butt, H. J.; Koynov, K. *Macromolecules* **2009**, *42* (22), 9183–9189.
(25) Braeken, E.; De Cremer, G.; Marsal, P.; Pèpe, G.; Müllen, K.; Vallée, R. A. L. *J. Am. Chem. Soc.* **2009**, *131* (34), 12201–12210.
(26) Lin, H. Z.; Tian, Y. X.; Zapadka, K.; Persson, G.; Thomsson, D.; Mirzov, O.; Larsson, P. O.; Widengren, J.; Scheblykin, I. G. *Nano Lett.* **2009**, *9* (12), 4456–4461.
(27) Lin, H. Z.; Hania, R. P.; Bloem, R.; Mirzov, O.; Thomsson, D.; Scheblykin, I. G. *Phys. Chem. Chem. Phys.* **2010**, *12* (37), 11770–11777.
(28) Bolinger, J. C.; Traub, M. C.; Adachi, T.; Barbara, P. F. *Science* **2011**, *331* (6017), 565–567.
(29) Flier, B. M. I.; Baier, M.; Huber, J.; Müllen, K.; Mecking, S.; Zumbusch, A.; Wöll, D. *Phys. Chem. Chem. Phys.* **2011**, *13* (5), 1770–1775.
(30) Suzuki, K.; Habuchi, S.; Vacha, M. *Chem. Phys. Lett.* **2011**, *505* (4−6), 157–160.
(31) Deschenes, L. A.; Bout, D. A. V. *J. Phys. Chem. B* **2002**, *106* (44), 11438–11445.
(32) Tomczak, N.; Vallée, R. A. L.; van Dijk, E. M. H. P.; García-Parajó, M.; Kuipers, L.; van Hulst, N. F.; Vancso, G. J. *Eur. Polym. J.* **2004**, *40* (5), 1001–1011.
(33) Schob, A.; Cichos, F.; Schuster, J.; von Borczyskowski, C. *Eur. Polym. J.* **2004**, *40* (5), 1019–1026.
(34) Zondervan, R.; Kulzer, F.; Berkhout, G. C. G.; Orrit, M. *Proc. Natl. Acad. Sci. U. S. A.* **2007**, *104* (31), 12628–12633.
(35) Adhikari, S.; Selmke, M.; Cichos, F. *Phys. Chem. Chem. Phys.* **2011**, *13* (5), 1849–1856.
(36) Uji-i, H.; Melnikov, S. M.; Deres, A.; Bergamini, G.; De Schryver, F.; Herrmann, A.; Müllen, K.; Enderlein, J.; Hofkens, J. *Polymer* **2006**, *47* (7), 2511–2518.
(37) Dedecker, P.; Muls, B.; Deres, A.; Uji-i, H.; Hotta, J.; Sliwa, M.; Soumillion, J. P.; Müllen, K.; Enderlein, J.; Hofkens, J. *Adv. Mater.* **2009**, *21* (10−11), 1079–1090.
(38) Böhmer, M.; Enderlein, J. *J. Opt. Soc. Am. B* **2003**, *20* (3), 554–559.
(39) Patra, D.; Gregor, I.; Enderlein, J. *J. Phys. Chem. A* **2004**, *108* (33), 6836–6841.
(40) Zheng, Z. L.; Kuang, F. Y.; Zhao, J. *Macromolecules* **2010**, *43* (7), 3165–3168.
(41) Habuchi, S.; Oba, T.; Vacha, M. *Phys. Chem. Chem. Phys.* **2011**, *13* (15), 6970–6976.
(42) Hofkens, J.; Vosch, T.; Maus, M.; Köhn, F.; Cotlet, M.; Weil, T.; Herrmann, A.; Müllen, K.; De Schryver, F. C. *Chem. Phys. Lett.* **2001**, *333* (3−4), 255–263.
(43) Weil, T.; Vosch, T.; Hofkens, J.; Peneva, K.; Müllen, K. *Angew. Chem., Int. Ed.* **2010**, *49* (48), 9068–9093.
(44) Lu, C. Y.; Vanden Bout, D. A. *J. Chem. Phys.* **2006**, *125* (12), xxxx.
(45) Lu, C. Y.; Bout, D. A. V. *J. Chem. Phys.* **2008**, *128* (24), xxxx.
(46) Krause, S.; Aramendia, P. F.; Täuber, D.; von Borczyskowski, C. *Phys. Chem. Chem. Phys.* **2011**, *13* (5), 1754–1761.
(47) Ferry, J. D. *Viscoelastic Properties of Polymers*; Wiley: New York, 1980.
(48) Zangi, R.; Mackowiak, S. A.; Kaufman, L. J. *J. Chem. Phys.* **2007**, *126* (10), xxxx.